other than the molecular conformation, however, so that the observed solvent effects cannot be ascribed to any single factor. The thermodynamic driving forces, diffusion coefficients, and degree of ion-pairing will all be affected by solvent polarity and could contribute toward the observed rates of CS and CR.

Acknowledgment. We thank the SERC and the Japanese Ministry of Education, Science and Culture for financial support of this work. The Center for Fast Kinetics Research is supported jointly by the Biotechnology Research Resources Program of the NIH (Grant RR00886) and by the University of Texas at Austin.

Internal Energy Effects on Ion-Neutral Complexes from Unimolecular Dissociation of *n*-Propyl Phenyl Ether Radical Cations

Eric L. Chronister and Thomas Hellman Morton*

Contribution from the Department of Chemistry, University of California, Riverside, California 92521-0403. *Received March 8, 1989*

Abstract: The aliphatic portions of many alkyl phenyl ethers rearrange in the course of mass spectrometric fragmentation. Decomposition of the molecular ion of deuterated *n*-propyl phenyl ether has been examined in two energy regimes, near threshold by MIKES and at higher energy by resonant two-photon ionization followed by photodecomposition. Formation of phenol molecular ions is the predominant fragmentation pathway, and examination of *n*-propyl-2,2-d_2 (β-d_2) and *n*-propyl-1,1,3,3,3-d_5 (α,γ-d_5) phenyl ethers shows that the reaction proceeds via intermediate [isopropyl cation phenoxy radical] ion-neutral complexes in both regimes. In the photoionization/photodecomposition experiment the hydrogens within the isopropyl moiety become completely scrambled, while in the MIKES experiment decomposition of the ion-neutral complex via proton transfer occurs 3.7 times faster than scrambling of the alkyl hydrogens. A simplified density-of-states model is presented to describe the dependence of ion-neutral complex formation upon internal energy. Calculations based on this model give a qualitative result that agrees with experiment, namely that ion-neutral complex formation is more probable than simple bond fission.

An ion-neutral complex is a noncovalently bound aggregate of an ion with one or more neutral molecules. Such species are formed as transient intermediates in the unimolecular decomposition of a variety of gaseous ions, a subject that has been recently reviewed.[1] Because the highly directional nature of covalent or hydrogen bonding is absent, an ion-neutral complex possesses internal rotor degrees of freedom that do not exist in the covalently bound precursor. Equation 1 schematically depicts two of these internal degrees of freedom, bending vibrations of the R-Y bond of the covalent precursor RY^+ that become internal rotations of the ion-neutral complex $[R^+\ Y]$.

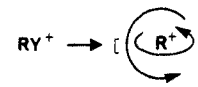

(1)

A series of experiments published in 1980 demonstrated that ion-neutral complexes are intermediates in the mass spectrometric decompositions of primary alkyl phenyl ethers.[2] This provided an explanation for several otherwise perplexing results. For instance, Benoit and Harrison had reported in 1976[3] that molecular ions of *n*-propyl phenyl ether decompose to the phenol molecular ion and that the itinerant hydrogen comes from all three positions of the alkyl chain in nearly statistical proportions. The interpretation of this result in terms of an intermediate ion-neutral complex is shown in eq 2. Rapid scrambling of the hydrogens

$$CH_3CH_2CH_2OPh \xrightarrow{-e^-} [CH_3CHCH_3^+ \quad PhO^\bullet] \xrightarrow{k} PhOH^{\bullet+} + C_3H_6 \quad (2)$$

in the isopropyl cation[4] accounts for the indistinguishability of the alkyl hydrogens prior to proton transfer to the phenoxy radical, a reaction that yields phenol$^{\bullet+}$ as the most prominent peak in the mass spectrum. Many alternatives have been ruled out, and eq 2 depicts a pathway for randomization of the alkyl hydrogens that is consistent with the distributions of hydrocarbon isomers expelled by larger alkyl phenyl ether molecular ions.

Lately a group at the Ecole Polytechnique has raised the question as to whether the mechanism of alkyl phenyl ether decompositions might change as a function of internal energy.[5] Specifically, they suggest that elimination of phenol molecular ion via a six-member cyclic transition state, as represented schematically in eq 3, or a concerted hydrogen transfer from

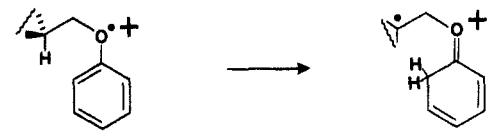

(3)

carbon to oxygen could contribute a major pathway in some cases at very low internal energies. While it is entirely plausible that two mechanisms might compete with one another, we have presented arguments against there being a substantial change in mechanism as a function of internal energy.[6]

In order to probe this issue more deeply we report here the decomposition of deuterated analogues of *n*-propyl phenyl ether under two regimes. For a low-energy regime we have chosen to study metastable parent ions that live 10^{-6} s prior to fragmentation by using the MIKES (Metastable Ion Kinetic Energy Spectroscopy) technique on a reverse Nier-Johnson geometry mass spectrometer. Electron impact produces ions with a wide and, as yet, poorly defined distribution of internal energies. Only the

(1) McAdoo, D. J. *Mass Spectrometry Rev.* **1988**, *7*, 363-393.
(2) Morton, T. H. *J. Am. Chem. Soc.* **1980**, *102*, 1596-1602.
(3) Benoit, F. M.; Harrison, A. G. *Org. Mass Spectrom.* **1976**, *11*, 599-608.
(4) McAdoo, D. J.; McLafferty, F. W.; Bente, III, P. F. *J. Am. Chem. Soc.* **1972**, *94*, 2027-2033.
(5) Sozzi, G.; Audier, H. E.; Morgues, P.; Millet, A. *Org. Mass Spectrom.* **1987**, *22*, 746-747.
(6) Kondrat, R. W.; Morton, T. H. *Org. Mass Spectrom.* **1988**, *23*, 555-557.

0002-7863/90/1512-133$02.50/0

ions seen in the MIKES, which represent the end of that distribution close to threshold, can be said to have a defined range of internal energies. For a high-energy distribution we have used photolysis of molecular ions generated by resonant two-photon ionization in a time of flight mass spectrometer. In this photoionization/photodecomposition experiment parent ions are produced when the neutral precursor (at a pressure in the range 10^{-6}–10^{-5} Torr) absorbs two 266-nm photons. A short time later (10^{-10} s) a third photon, 532 nm, is absorbed, as portrayed by eq 4, and the ensuing fragmentation is monitored. Under these

$$\begin{array}{l} M \xrightarrow{266\text{ nm}} M^{*} \xrightarrow{266\text{ nm}} M^{**} \xrightarrow{532\text{ nm}} \text{fragments} \\ \qquad\qquad\qquad\quad -e^{-}\big\downarrow 1/\tau \\ \qquad\qquad\qquad\quad M^{\bullet+} \xrightarrow{532\text{ nm}} \text{fragments} \end{array} \qquad (4)$$

conditions only the molecular ion, $M^{\bullet+}$, is formed by the 266-nm absorption. We assume that the interval between the UV pulse and the visible pulse is not much shorter than the time, τ, required for a preionizing state (represented as M**) to eject an electron. The internal energy content of the ions that subsequently absorb a 532-nm photon is at least 2.4 eV but no greater than the combined energy of two 266-nm photon and one 532-nm photon (12.0 eV) minus the ionization potential. Since simple alkyl phenyl ethers have adiabatic IP's of 8.0–8.2 eV,[2] the maximum energy content of the molecular ions that decompose is 4 eV, of which a portion is carried away by the ejected electron.

Experimental Section

Materials. Deuterated *n*-propyl phenyl ethers were prepared from phenoxyacetone (Aldrich; freshly distilled before use) rather than by Williamson ether synthesis, so as to avoid ring-alkylated phenols that often arise as impurities in the latter method. *n*-Propyl-*2,2-d*$_2$ phenyl ether (β-d_2) was synthesized by reduction of phenoxyacetone with lithium aluminum deuteride, conversion to the tosylate, and reduction with lithium aluminum deuteride/lithium deuteride.[7] Phenoxyacetone-*1,1,3,3,3-d*$_5$ was prepared from phenoxyacetone by three repetitive exchanges with 0.2 M NaOD in D_2O followed by distillation, reduction with lithium aluminum hydride, conversion to the tosylate, and reduction with lithium aluminum hydride/lithium hydride. Both compounds were distilled twice (57–60 °C/3 Torr) before use.

Mass Spectrometric Measurements. MIKES experiments were performed with 70 eV electron impact on a VG ZAB-2F double sector (B-E) mass spectrometer at UCR.[6] Resonant two-photon ionization/dissociation mass spectra were obtained at UCLA by using the second and fourth harmonic outputs of a mode-locked Nd:YAG laser producing 2×10^{-11} s pulses at 10-Hz repetition rate (Quantel YG-471) with apparatus that has been previously described.[8] The 266-nm resonant pulse was adjusted to be about 10 μJ/pulse, while the 532-nm excitation pulses were kept at approximately 0.5 mJ/pulse. The optical setup allows the 532-nm pulse to be adjustably delayed, but for the results presented, a fixed delay of less than 100 ps relative to the photodissociating 266 nm pulse was used. A mass spectrum of the resulting fragment ions was obtained with use of a Wiley–McLaren type time-of-flight (TOF) mass spectrometer. The mass spectrometer was differentially pumped to maintain sample pressures of 10^{-5} Torr with the field free drift region pressure $\leq 2 \times 10^{-7}$ Torr. A two plate microchannel analyzer was used as the ion detector with a further 100-fold amplification by a video amplifier (Pacific Precision Instruments). A transient digitizer (Biomation) was used to capture the TOF mass spectrum after each laser shot, and an LSI-11 microcomputer was used to average 100 mass spectra.

Computational Methods. Optimized geometries for isopropyl cation and phenoxy radical were calculated by using the STO-3G basis set by means of the GAUSSIAN 82[9] program on the Cray X-MP/48 at the San Diego Supercomputing Center. Electronic energies for 62 different separations and orientations of the ion–neutral complex in the domain r = 7–15 Å were computed by using these geometries of the ion and molecule. The ion–neutral potential energy as a function of the center-of-mass separation (r) and the orientation angles of the isopropyl cation (angles ψ and ω) were fitted by standard least-squares procedures. The potential energy as a function of the orientation of the phenoxy radical (angles θ and ϕ) at a given separation was fitted by Fourier analysis, and the hindered rotor levels computed using a basis set of 100 trigonometric functions.[10] Harmonic oscillator densities of states and transition-state fluxes were computed semiclassically[11] using experimental vibrational frequencies for phenoxy radical[12] and SCF calculated normal modes for isopropyl cation (C_{2v} geometry; 3-21G frequencies scaled by a factor of 0.9).[13]

Results

We have examined two deuterated analogues of *n*-propyl phenyl ether, $CH_3CD_2CH_2OPh$ (β-d_2) and $CD_3CH_2CD_2OPh$ (α,γ-d_5). Formation of ion–neutral complexes of isopropyl cation and phenoxy radical, [*i*-Pr^+ PhO$^\bullet$], from these precursors will give characteristic distributions of isotopic label in the phenol molecular ion produced by mass spectrometric decomposition. For example, the α,γ-d_5 precursor should yield, initially, the complex of ion **1** with $C_6H_5O^\bullet$. If there is sufficient internal energy, **1** will undergo scrambling as depicted in eq 5 to yield a statistical mixture

$$\underset{\mathbf{1}}{CD_2HCHCD_3^+} \xrightarrow{k'} \underset{\mathbf{2}}{CD_2HCDCD_2H^+} \quad \text{or} \quad \underset{\mathbf{3}}{CD_3CDCDH_2^+} \qquad (5)$$

(neglecting isotope effects) of **1**:**2**:**3** = 2:3:2. The ion–neutral complex [**1** PhO$^\bullet$] should yield $PhOD^{\bullet+}$ (m/z 95) and $PhOH^{\bullet+}$ (m/z 94) in a statistical ratio (neglecting isotope effects) of 5:1, since only the methyl groups can donate protons from an isopropyl cation. Complexes containing the completely scrambled isopropyl cation should yield the two daughter ions in a statistical ratio of 2.5:1. If the process represented by eq 3 were the sole pathway, no $PhOD^{\bullet+}$ would be expected from α,γ-d_5.

Representative mass spectra from the photoionization/photodecomposition experiment are shown in Figure 1. The $PhOD^{\bullet+}/PhOH^{\bullet+}$ ratios from β-d_2 (98.5% d_2, 1.5% d_1 impurity) and α,γ-d_5 (93%-d_5, 7%-d_4 impurity) are 0.31 (SD = 0.02) and 2.11 (SD = 0.23), respectively. These data can be analyzed in a straightforward fashion to extract the average isotope effect, k_H/k_D, and the proportion of hydrogen transfer from the positions that were originally β and originally α and γ.[2] The results of this kinetic analysis (after correction for natural abundance ^{13}C and incomplete deuteration) give $k_H/k_D = 1.2 \pm 0.1$ and $k_{\alpha\gamma}/k_\beta = 2.5 \pm 0.3$. In other words, within the experimental uncertainty (±10%, due to the shot-to-shot variation of laser pulse intensity) the proportion of hydrogen transfer (neglecting isotope effects) from original position β versus that from original positions α and γ is consistent with the ion–neutral complex mechanism drawn in eq 2, in which complete scrambling takes place in the isopropyl cation. This agrees with the results previously reported by Benoit and Harrison with use of electron impact.[3]

The results of the MIKES experiment are shown in Figure 2. Here the $PhOD^{\bullet+}$:$PhOH^{\bullet+}$ ratios from β-d_2 and from α,γ-d_5, 0.20 (SD = 0.01) and 3.8 (SD = 0.2), yield the same value for k_H/k_D, 1.15 ± 0.05, but a value for $k_{\alpha\gamma}/k_\beta$, 4.3, that is different from photoionization/photodecomposition. This result admits of more than one interpretation, of which the following two possibilities represent limiting cases. Either the reaction in eq 2 takes place with incomplete scrambling of the hydrogens in the isopropyl group, giving a ratio between $k_{\alpha\gamma}/k_\beta = 5$ (expected for no scrambling) and $k_{\alpha\gamma}/k_\beta = 2.5$ (expected for complete scrambling), or else the ion–neutral complex intervenes entirely without scrambling but is in competition with a small proportion of decomposition (<15%) that takes place via the pathway shown in

(7) Helmkamp, G. K.; Rickborn, B. *J. Org. Chem.* **1957**, *22*, 479–482.
(8) Gobeli, D. A.; Morgan, J. R.; St. Pierre, R. J.; El Sayed, M. A. *J. Phys. Chem.* **1984**, *88*, 178–181.
(9) Binkley, J. S.; Frisch, M. J.; DeFrees, D. J.; Raghavachari, K.; Whiteside, R. A.; Schlegel, H. B.; Fleuder, E. M.; Pople, J. A. GAUSSIAN 82, Department of Chemistry, Carnegie-Mellon University, Pittsburgh, PA.
(10) Lewis, J. D.; Chao, T. H.; Laane, J. *J. Mol. Struct.* **1972**, *12*, 427–499. We are grateful to Professor David F. Bocian for providing the computer program for these calculations.
(11) Using the program RRKM by W. L. Hase and D. L. Bunker (QCPE234).
(12) Tripathi, G. N. R.; Schuler, R. H. *J. Chem. Phys.* **1984**, *81*, 113–121. Where radical frequencies were unavailable, values for phenol were used taken from Tripathi, G. N. R. *J. Chem. Phys.* **1975**, *71*, 4025.
(13) Stams, D. A.; Johri, K. K.; Morton, T. H. *J. Am. Chem. Soc.* **1988**, *110*, 699–706.

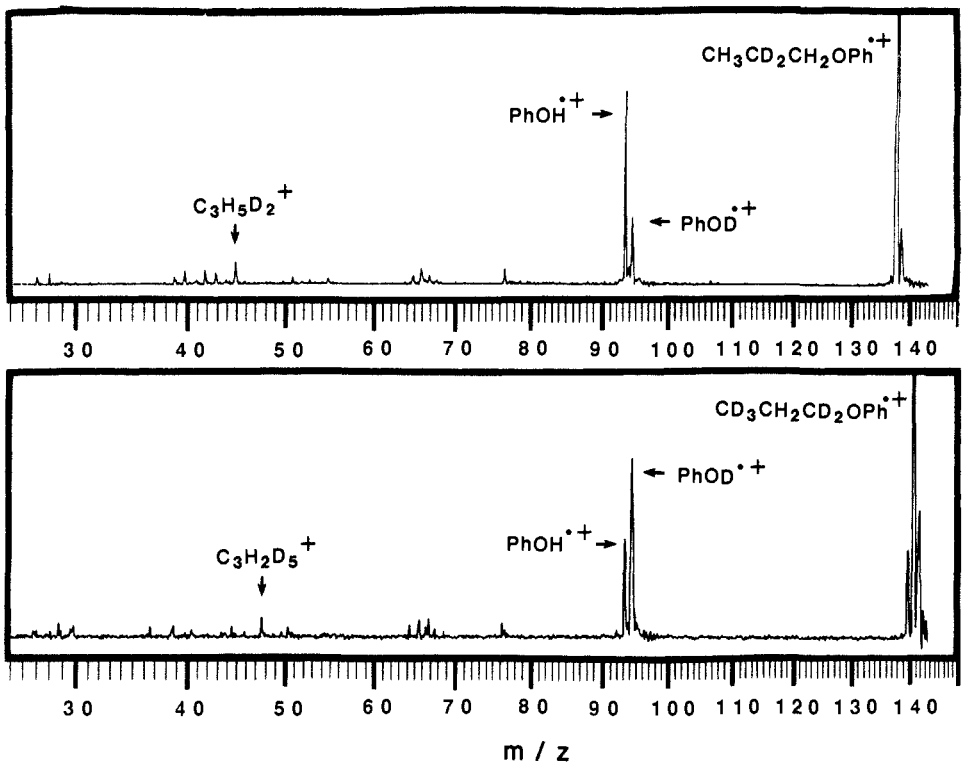

Figure 1. Resonant two-photon ionization/photodecomposition time-of-flight (R2PI/PD/TOF) mass spectra of deuterated *n*-propyl phenyl ethers. Each spectrum is the sum of 100 transients from a 10 μJ 266-nm pulse followed by a 0.5 mJ 532-nm pulse (if the 532-nm pulse is omitted, only molecular ions are seen). Although $M^{\bullet+}$ peaks (m/z 138 from d_2, m/z 141 from d_5) are offscale, the amount of d_4 impurity in the d_5 compound can be gauged by comparing the intensities of m/z 140 and the natural abundance ^{13}C peak at m/z 142.

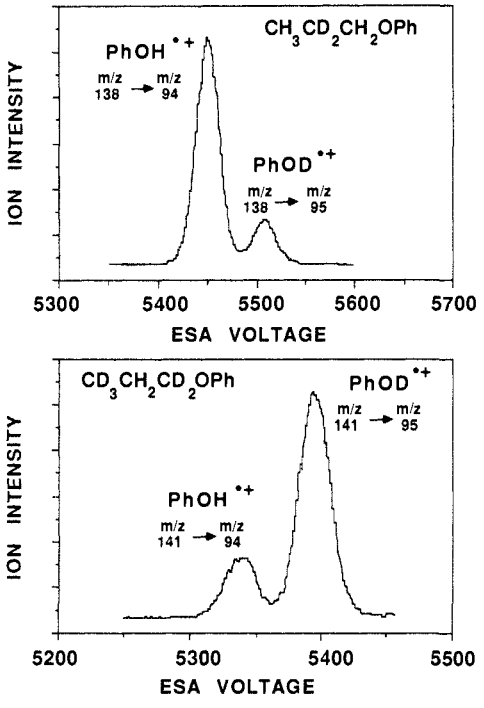

Figure 2. MIKES peaks corresponding to propene expulsion from d_2 and d_5 *n*-propyl phenyl ether molecular ions (70 eV electron impact ionization). The magnetic sector resolution was 2000. The main beam energy was 8 kV, and the electrostatic analyzer was scanned to observe metastable ions in the second field-free region. The next most intense ion in both MIKES spectra corresponds to $M^{\bullet+} \rightarrow m/z$ 77 and is <5% the intensity of the $M^{\bullet+} \rightarrow$ phenol$^{\bullet+}$ peaks. No $M^{\bullet+} \rightarrow m/z$ 78 is detected.

eq 3. In any event, reaction 2 represents the dominant pathway, where the isopropyl cation scrambles slowly or not at all.

The translational kinetic energy release, $T_{0.5}$ = 0.023 eV, is the same as previously reported by Benoit and Harrison for undeuterated phenyl propyl ether.[3] Field ionization kinetics (FIK) of variously deuterated propyl phenyl ether molecular ions[14] show that decomposition to phenol$^{\bullet+}$ is a fast process, so it does not seem likely that the MIKES represents high-energy ions that experience large kinetic shifts. McAdoo et al.[4] have shown that the rate of hydrogen scrambling in free isopropyl cations generated from *n*-propyl precursors is highly dependent upon internal energy and that at sufficiently low energies scrambling is not observed on the millisecond time scale. Therefore one should expect to see incomplete scrambling in the cation portion of an ion–neutral complex at low internal energies. The data shown in Figure 2 correspond to a mixture of 82% unscrambled isopropyl cation with 18% statistically scrambled cation. If fit to a kinetic expression in which the reaction $\mathbf{1} \xrightleftharpoons{k} \mathbf{1} + \mathbf{2} + \mathbf{3}$ (in statistical proportions) competes with [**1** PhO$^{\bullet}$] $\xrightarrow{k}$ phenol$^{\bullet+}$, the data correspond to k'/k = 3.7.

Table I. Electronic Energies (in kJ mol^{-1} Relative to Infinite Separation) of Diatomics Held with Their Centers of Mass 6 Å Away from Li^+[a]

	Li^+···F–H	Li^+···O–H$^{\bullet}$	Li^+···OC
HF/STO-3G	−8.7	−9.1	−3.2
HF/3-21G	−16.2	−15.8	−9.2
HF/6-31G	−14.3	−16.7	−9.3
HF/6-31G*	−13.8	−13.9	−5.9
HF/6-31G**	−13.6	−13.8	"
HF/6-311G**	−14.0	−14.0	−5.2
MP3/6-311G**	−13.8	−13.7	−4.2

[a] Diatomic bond lengths were optimized at the level at which the computation was performed, and the three-center systems were fixed in the linear geometries shown.

Calculations

Computations were performed to test a simple model and assess a lower limit for ion–neutral complex formation. The potential energy surface of the [isopropyl cation phenoxy radical] ion–neutral complex as a function of the variables r, θ, ϕ, ψ, and ω (shown in Figure 3) was computed by using the STO-3G basis

(14) (a) Borchers, F.; Levsen, K.; Beckey, H. D. *Int. J. Mass Spectrom. Ion Phys.* **1976**, *21*, 125–132. (b) Beckey, H. D.; Levsen, K.; Derrick, P. J. *Org. Mass. Spectrom.* **1976**, *11*, 835–837.

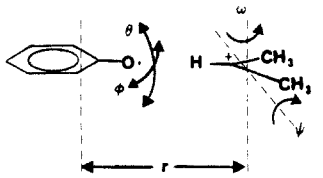

Figure 3. Ion–neutral complex between phenoxy radical and isopropyl cation showing the angular displacements (θ and ϕ) treated as librations and the three coordinates (r, ψ, and ω) of the point dipole in the field of the ion that are used in eq 6. All four angular displacements are treated as free rotors in the transition state for simple C–O bond fission.

Table II. Potential Energy for [Isopropyl Cation Phenoxy Radical][a]

r =	7 Å	8 Å	10 Å	12 Å	15 Å
$V(\theta = \phi = 0)$	−21.0	−13.6	−7.3	−4.6	−2.6
$V(\theta = 90°, \phi = 0)$	−0.7	−0.5	−0.2	−0.1	−0.03
$V(\theta = 0, \phi = 90°)$	1.9	1.5	0.9	0.6	0.4
$V(180°)$[b]	6.3	5.2	3.7	2.7	1.5
$\nu_\theta(cm^{-1})$	23.1	19.2	12.1	8.8	6.6
$\nu_\phi(cm^{-1})$	28.1	23.3	14.7	10.6	8.0

[a] For $J = 0$ at $\psi = \omega = 0$ as a function of θ and ϕ (in kJ/mol) and vibrational frequencies (ν_θ, ν_ϕ) calculated for the corresponding librations. [b] $V(\theta = 180°, \phi = 0) = V(\theta = 0, \phi = 180°)$.

set. We are concerned with geometries where the ion and neutral are separated by distances r that are much greater than the equilibrium value. The justification for using STO-3G is summarized by Table I, which tabulates the potential energies of Li^+ held 6 Å away from three different diatomics as a function of basis set and computational level. As the results show, ab initio calculations, do not approach their limiting values until polarization functions are included. In every case STO-3G shows a weaker attraction than does any other computational level. Since the objective is to secure a lower limit for the probability of ion–neutral complex formation, a lower-bound estimate of the attractive potential at separations >6 Å is to be desired. SCF calculations with the STO-3G basis set appear to provide such estimates. Although some error is introduced by using center-of-mass interfragment distances, the ab initio potential energy function at $\theta = \phi = 0$ was found to be well fit by the expression in eq 6 (V in kJ mol^{-1}, r in Å).

$$-V(r,\psi,\omega) = [484.6 + 9.6\cos(\psi + \omega) - 10.55\cos 2\psi + 0.4\cos 2\omega]/r^2 + [20040 + 4318\cos(\psi + \omega) + 1970\cos 2\psi - 1549\cos 2\omega]/r^4 - h^2J(J+1)/8\pi^2\mu r^2 \quad (6)$$

The energetically most favorable geometry corresponds to $\theta = \phi = \psi = \omega = 0$, which is shown in Figure 3. At this geometry the potential as a function of r is very well fit by a permanent dipole/induced dipole potential where $\mu_E = 1.67$ D and $\alpha = 35.7$ $Å^3$. At a distance $r_1 = 8$ Å rotation by 180° about angle ψ represents the highest barrier to the isopropyl cation as an internal rotor, with a barrier height of 2.5 kJ mol^{-1}.

The potential energy at $\phi = \psi = \omega = 0$ and $J = 0$ was computed at $r = 7$, 8, 10, 12, and 15 Å for $\theta = 0$, 30, 60, 90, 120, 150, and 180° and was fitted by Fourier analysis to a six-term cosine function,

$$\sum_{n=0}^{6} V_n \cos n\theta$$

at each value of r. Hindered internal rotor energy levels were calculated at each value of r, and the spacings between the first two levels are summarized in Table II.

Discussion

Four decomposition processes dominate the resonant two-photon ionization/photodecomposition spectra shown in Figure 1. The most abundant fragment ions are phenol molecular ions (m/z 94 and 95), which arise as shown by eq 2. Simple C–O bond fission contributes propyl cations, the next most abundant fragments, m/z 45 from β-d_2 and m/z 48 from α,γ-d_5 (as well as allylic cations at lower masses from subsequent hydrogen expulsion). Formal loss of an alkoxy radical yields the third most abundant ion at m/z 77. Since this ion is barely detectable in the mass spectrum of phenol but is seen in phenyl ethers, it must come from direct fragmentation of phenyl propyl ether molecular ions. The daughter ions at m/z 66–67 represent expulsion of carbon monoxide from the m/z 94 and 95 ions and correspond to decompositions of excited phenol ions, which have been widely discussed by other investigators.[15] These ions, the allylic ions, and all of the additional, smaller peaks can be ascribed to multiphoton decompositions and will not be further discussed.

We shall focus on the relative proportions of the two most prevalent fragmentation pathways, simple fission and eq 2. In both cases sp^3 C–O bond cleavage constitutes the first step. In the less frequent process, the two resulting fragments separate to a large enough distance that the alkyl cation from simple fission is detected. More often the fragments do not escape from one another, and an ion–molecule reaction (proton transfer) takes place between the alkyl cation and phenoxy radical.

The reaction coordinate for such a decomposition is complicated. Formation of phenol$^{\bullet+}$ has an observed appearance potential 1.0 eV above the thermodynamic threshold,[17] which represents an upper bound for the barrier to rearrangement from 1-propyl to isopropyl that accompanies cleavage of the sp^3 C–O bond. The small kinetic energy release, $T_{0.5} = 0.023$ eV, can be interpreted as evidence for an intermediate (which we believe to be an ion–neutral complex) subsequent to the barrier. Figure 4 schematically depicts two different sections along the potential energy surface, which intersect in the vicinity of the ion–neutral complex. The solid line represents the potential energy along the reaction coordinate for direct formation of propene and phenol$^{\bullet+}$, where the barrier height is taken to have the value (100 kJ mol^{-1} greater than the thermodynamic barrier) from the appearance potential measurement (neglecting kinetic shifts). The dashed line represents the simple bond cleavage of the molecular ion of phenyl isopropyl ether, for which we assume there is no reverse activation barrier. We propose that the ion–neutral complex exists where the sp^3 C–O bond distance is more extended than it is at the intersection of these two superimposed curves. We model the reaction as though the most probable pathway (going from left to right) corresponds to passing from the solid curve onto the dashed curve in the vicinity of their intersection. The ion–neutral complex sojourns on the dashed curve (with only a small probability of continuing all the way to the right) before crossing back to the solid curve and then going to the right to yield propene and phenol$^{\bullet+}$.

Our model would not be useful if it depended upon potential energy barriers between the ion–neutral complex and its covalent precursor, since there is probably no potential energy barrier to collapse of the complex to an isomeric covalent molecular ion (i.e. that of isopropyl phenyl ether in Figure 4). The model therefore considers only product-like critical configurations and weighs the relative probabilities that a precursor, $ROPh^{\bullet+}$, will undergo simple fission to free R^+ and PhO$^\bullet$ versus cleavage to form the ion–neutral complex [R^+ PhO$^\bullet$]. To evaluate the weights of these two channels we need only consider the portion of the dashed curve in Figure 4 that is to the right of the crossing of the two curves. Figure 5 portrays the pertinent parameters along a generalized C–O stretch coordinate. We consider the number of vibrational states in the product channel that corresponds to simple fission, $G_{3N-7}(E^* - E_o)$, when the precursor parent ion has internal energy E^* and a dissociation barrier E_o. We compare this with the number of states in the product channel that corresponds to formation of an ion–neutral complex. This treatment will make use of simple approximations that yield an upper bound for G_{3N-7} and a lower bound for the number of states corresponding to an

(15) (a) Lifshitz, C.; Gefen, S.; Arakawa, R. *J. Phys. Chem.* **1984**, *88*, 4242–4246. (b) Malinovich, Y.; Lifshitz, C. *J. Phys. Chem.* **1986**, *90*, 4311–4317.

(16) Forst, W. *Theory of Unimolecular Reactions*; Academic Press: New York, 1973.

(17) Blanchette, M. C.; Holmes, J. L.; Lossing, F. P. *Org. Mass Spectrom.* **1989**, *24*, 673–678.

ion–neutral complex. For dissociation along the C–O stretching coordinate equal weighting of all states leads to the familiar RRKM expression

$$G_{3N-7}(E^* - E_o) = \int_0^{E^*-E_o} \rho_{3N-7}(E)\, dE \qquad (7)$$

where ρ_{3N-7} designates the density of states for a product-like transition state.[16] For present purposes the $3N-7$ degrees of freedom include the internal degrees of freedom of R^+, the internal degrees of freedom of PhO•, and five rotational degrees of freedom of the two fragments that will be treated as free rotors.

Formation of an ion–neutral complex proceeds along the same reaction coordinate as simple fission, but this motion remains bound. Beyond some limit of C–O extension we assume that the internal degrees of freedom corresponding to motion of the ion relative to the neutral are no longer coupled to the other internal degrees of freedom (i.e., energy flow between this motion and the other internal degrees takes place on a time scale longer than the lifetime of the ion–neutral complex). The distance at which this decoupling occurs is much longer than bonding distance, and we feel that it is safe to suppose that, at a C–O bond length $r_1 > 5$ Å, the [R^+ PhO•] ion–neutral complex is in this region. If we were not to make this assumption we would find that the density of states (which we designate as ρ'_{3N-6}) corresponding to ion–neutral complexes is so much smaller (<1%) than the density of states of covalently bound propyl phenyl ether molecular ions that the presumption of rapid energy exchange among all internal degrees of freedom would predict ion–neutral complexes to make a negligible contribution among freely equilibrating structures.

Many of the internal degrees of freedom of [R^+ PhO•] are the same as for the product-like transition state for simple fission: the vibrations of R^+, the vibrations of PhO•, and the rotation about the C–O bond axis. Two additional degrees of freedom correspond to rigid motions of the phenoxy radical, which are treated as a pair of librations (since PhO• has a permanent dipole moment that leads to a net repulsive potential when it is rotated 180° relative to R^+). Together all of these degrees of freedom contribute to a density of states that we shall designate as ρ'_{3N-9}. Klippenstein and Marcus have presented a general treatment for the remaining degrees of freedom.[18] We describe here, however, a specific approach for ion–neutral complexes. The remaining three degrees of freedom correspond to the two angular displacements depicted in eq 1 (angles designated as ψ and ω in Figure 3) as well as the distance (r) between the ion and the neutral. The potential is portrayed in terms of a charge located at the center of mass of R^+ interacting with the permanent and induced dipoles of PhO•.

The Schrödinger equation for such a potential does not have a closed-form solution. We can, however, secure a useful estimate of the number of states, W, from the Bohr–Sommerfeld (semiclassical) formulation[19] by using the potential energy V from eq 6.

$$W \approx \frac{8\pi\sqrt{2\mu^3}}{3h^3} \int_{r_1}^{r_2} \int_0^{\pi} \int_0^{2\pi} (-V)^{3/2} r^2 \sin\psi\, dr\, d\psi\, d\omega \qquad (8)$$

The C–O distances considered are large enough that we shall use separations between the centers of mass of the two fragments as the limits of integration r_1 and r_2. The reduced mass μ is simply the two-body value for the ion and the neutral. The number of states that can lead to the ion–molecule complex is approximated by convolving ρ'_{3N-9} and the first derivative of W with respect to energy and then multiplying the resulting density of states, ρ'_{3N-6}, by an energy width ΔE.

$$\Delta E \rho'_{3N-6}(E^* - E_1) = \Delta E \int_0^{E_2-E_1} \frac{dW(x)}{dV} \rho'_{3N-9}(E^* - E_1 - x)\, dx \qquad (9)$$

(18) (a) Klippenstein, S. J.; Marcus, R. A. *J. Phys. Chem.* **1988**, *92*, 3105–3109. (b) Klippenstein, S. J.; Marcus, R. A. *J. Phys. Chem.* **1988**, *92*, 5412–5417.

(19) Landau, L. D.; Lifshitz, E. M. *Quantum Mechanics*; 3rd ed.; Pergamon Press: Oxford, 1977; pp 170–175.

Table III. Number of States for the Dissociation Product Channel, G_{3N-7}, and the Density of States, ρ'_{3N-6} (in States per cm^{-1} for the Interval $r_1 = 7$ Å, $r_2 = 15$ Å), of the [PhO• $C_3H_7^+$] Ion Neutral Complex[a]

	E^*		
	225	225	450
J	0	160	0
$E^* - E_0$	15	20	240
ρ'_{3N-6}	3.8×10^{12}	4.9×10^{12}	1.9×10^{27}
G_{3N-7}	6.3×10^{11}	4.2×10^{12}	1.5×10^{28}

[a] As a function of internal energy E^* (in kJ mol^{-1}) and rotational angular momentum quantum number J.

As noted above, this treatment does not demand that there be any potential energy barrier to ion–neutral complex formation. Here we estimate that the lower bound for the ratio $(\Delta E)(\rho'_{3N-6})/G_{3N-7}$ in the photodecomposition experiment is not far from unity. For decomposition of *n*-propyl phenyl ether radical cation to isopropyl cation plus phenoxy radical the experimental value of E_o is 210 ± 10 kJ mol^{-1}. This is based on a heat of formation of the parent molecular ion $\Delta H_f°(n\text{-PrOPh}^{+\bullet}) = 645$ kJ mol^{-1}, inferred from an estimated adiabatic ionization potential of *n*-PrOPh of 8.0 eV (bracketed by the published photoelectron spectra of its higher[2] and lower[20] homologues), and a heat of formation of phenoxy radical[21] of $\Delta H_f° = 56$ kJ mol^{-1}. The lower bound for E^* corresponds to absorption of a single 532-nm photon by the lowest vibrational state of *n*-$PrOPh^{+\bullet}$, $E^* \geq 225$ kJ mol^{-1}. We choose $r_1 = 7$ Å and $r_2 = 15$ Å to represent a region of the ion–neutral complex where covalent interaction between the two fragments is negligible and the electrostatic attraction is >2 kJ mol^{-1}. From a semiclassical calculation[18] we estimate that there are $W = 5.1 \times 10^6$ states corresponding to the ion–dipole potential in this region at $J = 0$. The convolution in eq 9 leads to the density of states ρ'_{3N-6} given in Table III.

Now consider the effects of rigid overall rotation. The effective values of E_o, E_1, and E_2 will all decrease: E_o most of all and E_2 least of all. *n*-Propyl phenyl ether is a near-prolate rigid rotator. The [isopropyl cation phenoxy radical] ion–neutral complex is also near-prolate, and the reaction coordinate for C–O bond dissociation corresponds to extension of the major axis. Therefore the centrifugal portion of the potential energy in eq 6 is treated as for a linear rigid rotator. If we assume that the *n*-propyl phenyl ether molecular ion has the thermal distribution of rotational angular momenta of its neutral precursor, then the most probable value of the angular momentum quantum number is on the order of $J = 75$, and 90% of the molecular ions will have $J \leq 160$. Substituting $J = 160$ into eq 6 and 8 gives $W = 3.4 \times 10^6$ states and, from eq 9, the density of states ρ'_{3N-6} in Table III.

The value of ΔE is at least equal to the homogeneous line width of the absorption, and, in any event, cannot be less than the uncertainty broadening of the 10^{-11} s laser pulse, 0.5 cm^{-1}. Therefore the number of states corresponding to an ion–neutral complex is $\Delta E \rho'_{3N-6} \geq 1.9 \times 10^{12}$ at $E^* = 225$ kJ mol^{-1} and $J = 0$. To estimate the relative probabilities of the two reaction channels we take the ratio of this to the number of states that correspond to complete dissociation G_{3N-7} (calculated by using eq 7), at the same value of E^* (which we consider to be an upper bound for the weighting of probability for simple fission, since we neglect corrections for "flexible" internal degrees of freedom[18] and for requirements imposed by conservation of angular momentum[22]). At the level of approximation where motions about

(20) (a) Dewar, P. S.; Ernstbrunner, E.; Gilmore, J. R.; Godfrey, M.; Mellor, J. M. *Tetrahedron* **1974**, *30*, 2455–2459. (b) Friege, H.; Klessinger, M. *Chem. Ber.* **1979**, *112*, 1614–1625.

(21) On the basis of a heat of formation of anisole of $\Delta H_f° = -68$ kJ mol^{-1} (Badoche, M. *Bull Soc. Chim. Fr.* **1941**, 212–220. Hales, J. L.; Lees, E. B.; Ruxton, D. J. *Trans. Faraday Soc.* **1967**, *63*, 1876–1879) and an sp^3 C–O bond dissociation energy of 266 kJ mol^{-1} (Suryan M. M.; Kafafi, S. A.; Stein, S. E. *J. Am. Chem. Soc.* **1989**, *111*, 1423–1429).

the angles θ, ϕ, ψ, and ω are treated as free internal rotations we get the values of G_{3N-7} in Table III.

These calculations show that ion–neutral complex formation should be more probable than simple fission. The ratio of probabilities is sensitive to the value of J, varying by a factor of 5 between $J = 0$ and $J = 160$. Since we do not know a priori what values of r_1 and r_2 should be used, we have chosen a domain (7–15 Å) that is probably much smaller than is spanned by the ion–neutral complex. Our object here is not to match the experimentally observed reaction channel ratio (which is >15:1 in favor of ion–neutral complex formation) but rather to examine how the ratio ought to change as a function of energy. For a low-energy regime we consider the MIKES region, where $E^* \leq E_0$ (in other words the appearance potential for phenol$^{\bullet+}$ is lower than the heat of formation of free PhO$^\bullet$ plus a free isopropyl cation). Here we expect (and observe) no simple fission. For a high-energy regime we consider $E^* = 450$ kJ mol^{-1}, which would correspond to the energy of a 266-nm photon (or two 532-nm photons). The values of ρ'_{3N-6} and G_{3N-7} in the higher energy regimes at $J = 0$ are summarized in Table III. If we take ΔE to be the same as for the 532-nm experiment the ratio $\Delta E\rho'_{3N-6}/G_{3N-7}$ in the high-energy regime is smaller by a factor of 48 than the value calculated for $E^* = 225$ kJ mol^{-1}.

For electron impact experiments, the value of ΔE is not defined by any laser excitation pulse width but rather by the lifetime of ion–neutral complexes prior to decomposition (which has been observed by field ionization kinetics to take place on the time scale of 10^{-10} s[14]). If we suppose that this reported measurement corresponds to a lower bound for the rate of proton transfer depicted in the second step of eq 2, then lifetime broadening will be on the order of $\Delta E \geq 0.05$ cm^{-1}. Even with this value of ΔE, the proportion of simple fission in an electron impact experiment where $E^* = 225$ kJ mol^{-1} ought to be less than the proportion of phenol$^{\bullet+}$. If we consider the effects of increasing the internal energy of the covalent precursor, the extent of simple fission would be expected to increase relative to ion–neutral complex formation (by nearly a factor of 50 for $E^* = 450$ kJ mol^{-1} versus $E^* = 225$ kJ mol^{-1}).

Once formed, the [R$^+$ PhO$^\bullet$] ion–neutral complex has the choice of three first-order reactions. It can collapse back to a covalent molecular ion (in the case of *n*-propyl phenyl ether this would yield an isomerized molecular ion of isopropyl phenyl ether), or it can fragment to free R$^+$ and phenoxy radical, or, finally, proton transfer can take place from the alkyl cation to the phenoxy radical. The Brønsted acid–base reaction between isopropyl cation to the phenoxy radical is 130 kJ mol^{-1} exothermic.[23] Since the product, phenol molecular ion, has been detected in previous FIK experiments at the shortest time scales accessible,[14] we suppose that the rate-limiting step under these conditions is the proton transfer. From previous studies of bimolecular reactions[24] we have concluded that the bottleneck in proton transfer from an alkyl cation to an *n*-donor base is not transit over a potential energy maximum. Instead, the rate of proton transfer is limited either by the alignment of the acidic C–H bond with the lone pair of the base or else by the breakup of the ion–neutral complex that contains the products. If we assume that the rate of proton transfer is therefore not very sensitive to internal energy, then the rate-limiting step in our MIKES experiments is formation of the ion–neutral complex.

The fact that there is a large reverse activation barrier accompanied by a small kinetic energy release[17] suggests that some kind of intermediate intervenes after a decomposing ion has surmounted the highest potential energy barrier to its decomposition. In principle the barrier could simply correspond to isomerization of *n*-propyl phenyl ether molecular ion to isopropyl phenyl ether molecular ion, with all subsequent chemistry coming from the latter ion. Alternatively, the barrier could correspond to isomerization to a distonic ion, such as the species shown to the right in eq 3. However it is not easy to see how these options by themselves could account for the observed hydrogen scrambling ratios.

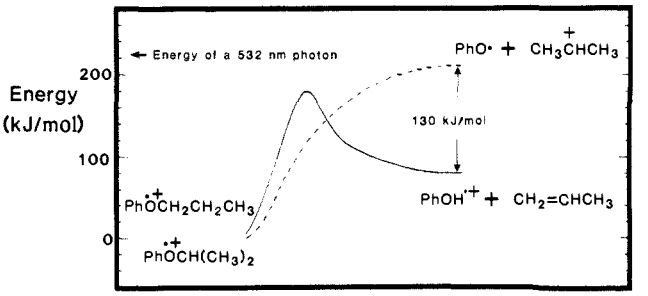

Figure 4. Reaction coordinate diagram for the decomposition of phenyl propyl ether molecular ions showing two cuts across the potential energy surface.

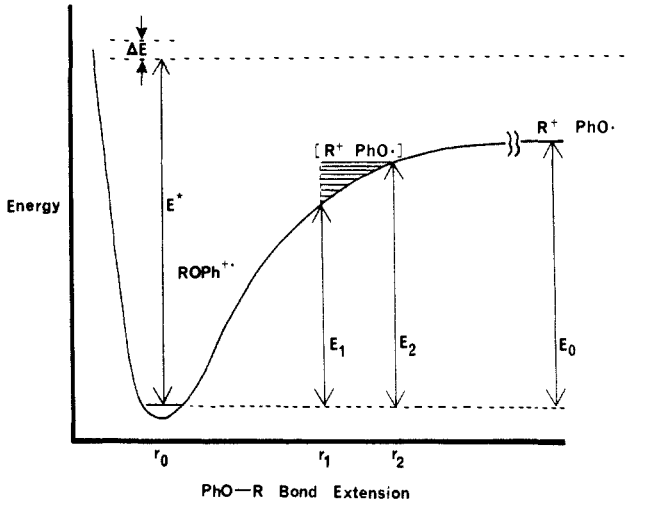

Figure 5. Section across the ROPh$^{\bullet+}$ potential surface corresponding to simple C–O bond fission (with no energy barrier to recombination at $J = 0$). E^* represents the internal energy of the molecular ion plus the energy of the last photon absorbed in reaction 4 (which, prior to reaction, is randomized among the internal degrees of freedom after internal conversion). The distances r_1 and r_2 correspond to the domain in which the fragments are bound by ion–dipole forces (Figure 3), with the range of internal energies $E^* - E_1$ and $E^* - E_2$, respectively. Energy transfer between other internal degrees of freedom and the degrees of freedom corresponding to r, ψ, and ω is assumed to be slow in this domain.

The intermediacy of ion–neutral complexes can be inferred from isotopic scrambling in the alkyl moiety prior to proton transfer. In our photoionization/photodecomposition experiments we cannot say for certain whether the scrambling has taken place before or after the absorption of the 532-nm photon, but comparison with the MIKES results suggests the latter. Absorption of the pair of 266-nm photons provides energy in excess of the thermodynamic threshold for fragmentation to phenol$^{\bullet+}$ ion but less than the reported activation barrier drawn in Figure 4. Only parent molecular ions are seen when the 532-nm pulse is omitted (provided that the laser power is sufficiently low). We assume that these ions (prior to the 532 nm pulse) have lower internal energy contents than the ions in the MIKES (which do decompose on the microsecond time scale but which do not exhibit complete scrambling). Since the energy of two 266-nm photons is lower than the reported appearance potential for decomposition, we infer that scrambling in the photoionization/photodecomposition experiment does not take place until after absorption of the 532-nm

(22) (a) Klots, C. E. *J. Chem. Phys.* **1964**, *41*, 117–122. (b) Klots, C. E. *Z. Naturforsch.* **1972**, *27a*, 553–561. (c) Klots, C. E. *J. Phys. Chem.* **1971**, *75*, 1526–1532. (d) Klots, C. E. *J. Chem. Phys.* **1976**, *64*, 4269–4275. (e) Illies, A. J.; Jarrold, M. F.; Bass, L. M.; Bowers, M. T. *J. Am. Chem. Soc.* **1983**, *105*, 5775–5781. (f) Jarrold, M. F.; Bass, L. M.; Kemper, P. R.; van Koppen, P. A. M.; Bowers, M. E. *J. Chem. Phys.* **1983**, *78*, 3756–3766. (g) Klots, C. E. *Acc. Chem. Res.* **1988**, *21*, 16–21.

(23) Lias, S. G.; Bartmess, J. E.; Liebman, J. F.; Holmes, J. L.; Levin, R. D.; Mallard, W. G. *J. Phys. Chem. Ref. Data* **1988**, *17*, Supplement 1.

(24) Redman, E. W.; Morton, T. H. *J. Am. Chem. Soc.* **1986**, *108*, 5701–5708.

photon. In any event, scrambling of isotopic label in the propyl moiety is complete within the 10^{-8} s time scale of the experiment (which is defined by TOF line widths).

The reported barrier height for decomposition is 100 kJ mol^{-1} above the thermodynamic threshold.[17] The ions that live 10^{-6} s prior to decomposition in the MIKES experiment probably have energy contents only slightly greater than this barrier height. This excess energy is somewhat greater than the activation energy for hydrogen scrambling in isopropyl cation.[25] The lifetime of the ion-neutral complex, once formed, may not be substantially longer than in the photoionization/photodecomposition experiment. In the MIKES, however, the rate of scrambling is 3.7 times slower than the rate of proton transfer.

The picture that emerges, both from our simplified theoretical model and from our experiments, is that the probability of intervention of an ion-neutral complex depends upon the energy content and rotational angular momentum of the precursor parent ion. The rate of hydrogen scrambling in the alkyl moiety within the ion-neutral complex, however, is also sensitive to internal energy content. Mechanistic studies that make use of internal energy variation must weigh these considerations.

Acknowledgment. We are grateful to Professor Mostafa El Sayed of UCLA, in whose laboratories the photodecomposition experiments were performed, to Dr. Diane Szaflarski for experimental assistance, and to Professor J. L. Holmes for providing a preprint of ref 17. Ab initio calculations were performed on the Cray X-MP/48 at the San Diego Supercomputing Center. The calculations in Table I were performed by Lohri Grishow and Shari Stockwell. This work was supported by NSF Grants CHE88-02086 and CHE84-12265.

Registry No. *n*-Propyl-2,2-d_2 phenyl ether, 61809-86-7; *n*-propyl-1,1,3,3,3-d_5 phenyl ether, 123676-11-9.

(25) Koch, W.; Liu, B.; Schleyer, P. v. R. *J. Am. Chem. Soc.* **1989**, *111*, 3479-3480.

"Salted" Iron Pentacarbonyl: Molecular Isolation in Alkali Halide Solids

Ewa S. Kirkor, Donald E. David, and Josef Michl*

Contribution from the Center for Structure and Reactivity, Department of Chemistry, The University of Texas at Austin, Austin, Texas 78712-1167. *Received April 29, 1988*

Abstract: The conditions for single-molecule isolation of iron pentacarbonyl by codeposition from vapor phase onto a cold substrate with excess alkali halide vapor have been established. The photochemistry of thus "salted" $Fe(CO)_5$ has been investigated as a function of the matrix ratio. In aggregated samples, $Fe_2(CO)_9$ is formed upon irradiation. In isolated samples, three primary photoprocesses have been documented: fragmentation with a gradual loss of CO ligands, oxidation, and reduction. The latter two events are attributed to interaction with light-induced defects and color centers. Similar reactions occur spontaneously after the initial deposition, already at very low temperatures, by the interaction of $Fe(CO)_5$ with defects and color centers formed during fast quenching in the deposition process. The photochemistry of salted $Fe(CO)_5$ was compared with that of $Fe(CO)_5$ adsorbed on alkali halide films. The properties of salted CO were also investigated.

Matrix isolation of organic materials in alkali halides and other room-temperature inorganic solids has recently elicited interest.[1] These mixed materials can be prepared by vapor codeposition.

A first communication[1a] reported that many nonionic compounds can be permanently incorporated into alkali halides ("salted") by cocondensation of the corresponding vapors onto a substrate cooled by liquid nitrogen (77 K) followed by warming the deposit to room temperature and evacuating it for a time amply adequate to remove all species located on the outer surfaces. Investigation of the photochemical behavior of salted iron pentacarbonyl, 2,2-dimesitylhexamethyltrisilane, anthracene, and 1-azidoadamantane showed that the guest molecules were aggregated in the two-component systems. A three-component system consisting of $Fe(CO)_5$ in an aliphatic hydrocarbon "padding" contained an alkali halide as a rigid matrix was also described. Coincorporation of the hydrocarbon allowed room-temperature single-molecule isolation of the $Fe(CO)_5$ guest, presumably in a hydrocarbon environment.

An East German group more recently also reported a preparation of this type of material.[1b] These workers used less volatile organic dopants and codeposited them with inorganic salts onto a room-temperature substrate. They proposed the name "norganics" for the resulting organic-inorganic composites.

The present study provides full details of our results for $Fe(CO)_5$ and reports progress along two lines. First, we have now attained the goal of isolating a nonionic compound in pure alkali halide matrices at the single-molecule dispersion level. Second, we have obtained evidence for processes in which color centers and defects in the alkali halide matrices act as chemical reagents toward a nonpolar dopant isolated in the matrix and compare these with their action on substrates merely adsorbed on the alkali halide surface.

Room-temperature matrix isolation in alkali halides and other relatively inert room-temperature solids is of interest for numerous reasons. It would offer convenient room-temperature storage for reactive or volatile molecules. It would permit low-temperature and high-temperature investigation of nonpolar and polar guest molecules in a highly unusual and yet possibly quite well defined environment, which may significantly alter their spectroscopic, photochemical, and oxidation-reduction behavior. It would permit an examination of temperature-dependent properties of the isolated molecules, including the study of the equilibrium population of low-lying excited states, normally negligible at the low temperatures characteristic of ordinary matrix isolation conditions, and the study of unimolecular reactions with sizable activation barriers. It would permit the probing of defects in the solid, such as color centers, through their interaction with the dopant. In a more general sense, the effects of the doping on the properties of the host solid, such as photoconductivity, dark conductivity, absorption, and spontaneous or stimulated emission, may be of even more

(1) (a) Kirkor, E.; Gebicki, J.; Phillips, D. R.; Michl, J. *J. Am. Chem. Soc.* **1986**, *108*, 7106. (b) Bötcher, H.; Vaupel, B.; Möbius, B. *J. Inf. Rec. Mater.* **1987**, *15*, 139. Vaupel, B.; Bötcher, H. *Z. Chem.* **1988**, *28*, 253. Böttcher, H.; Hertz, O.; Fritz, T. *Chem. Phys. Lett.* **1988**, *148*, 237. Böttcher, H.; Hertz, O.; Fox, M. A. *Chem. Phys. Lett.* **1989**, *160*, 121.

0002-7863/90/1512-139$02.50/0